Vol 12 No 2, February 2003
1009-1963/2003/12(02)/0159-05

Chinese Physics

© 2003 Chin. Phys. Soc.
and IOP Publishing Ltd

# Application of the second-order ground-state correlation and random-phase approximation on photoionization cross section of manganese*

Lu Peng-Fei(芦鹏飞), Liu Jin-Chao(刘锦超),
Yang Xiang-Dong(杨向东)†, and Ma Xiao-Guang(马晓光)

*Institute of Atomic and Molecular Physics, Sichuan University, Chengdu 610065, China*

(Received 12 July 2002; revised manuscript received 28 October 2002)

Using the many-body perturbation theory, we have calculated the photoionization cross section of 3p and 3d subshells of the neutral manganese, and discussed the second-order ground-state correlation and random-phase approximation correlations in detail. This is the first theoretical calculation for manganese as far as we know. Our calculated results are more consistent with the experimental results than those given by other methods in the literature.

**Keywords:** photoionization cross section, many-body perturbation theory, ground-state correlation, random-phase approximation

**PACC:** 3280, 3280F, 3380E

## 1. Introduction

The photoionization cross section of manganese has been the subject of many theoretical and experimental studies. Compared with the series of 3d transitional metal, manganese provides a convenient test for the photoionization dynamics because it has a half-filled 3d subshell and other filled subshells, thus simplifying theoretical calculations. It has a low vaporization temperature, this also simplifies experimental procedures. In 1989, Jiménez-Mier *et al*[1] completed a fairly elaborate experiment concerning the absolute partial photoionization cross section and the angular distribution parameter of 3d, 3p and 3s photoelectrons in the energy range of 50–300eV. However, the theoretical calculations of 3d and 3p partial cross sections[2] did not agree well with the experimental results. Recently, many-body perturbation theory(MBPT) is widely used to calculate cross sections of photoionization and resonance structure in atoms and ions.[3−6] In this paper, our main goal is to investigate the origin of the disagreement between experimental and theoretical studies and give better calculated results by using MBPT.

We present results for the 3d→ $k$f cross section, and the 3p and 3d partial cross sections of manganese in a wide energy range. For each subshell, we first consider the correlation from the lowest order to the second order of ground-state correlation (GSC) and random-phase approximation (RPA). Garvin *et al*[7] have calculated the 3p and 3d subshells of manganese, but they did not include and analyse the second-order correlations of GSC and RPA during the calculation.

## 2.Theory and method

Based on the electric-dipole approximation, the atomic photoionization cross section is

$$\sigma(\omega) = \frac{4\pi\omega}{c}\mathrm{Im}a(\omega), \tag{1}$$

where $\mathrm{Im}a(\omega)$ is the frequency-dependent polarizability. Atomic units are used throughout this paper.

Using MBPT, we express $\mathrm{Im}a(\omega)$ in dipole matrix elements as

$$Z_L = \left\langle \psi_\mathrm{f} \middle| \sum_{i=1}^{N} z_i \middle| \psi_0 \right\rangle \qquad \text{(length form)}, \tag{2}$$

$$Z_V = (E_0 - E_\mathrm{f})^{-1} \left\langle \psi_\mathrm{f} \middle| \sum_{i=1}^{N} \frac{\mathrm{d}}{\mathrm{d}z_i} \middle| \psi_0 \right\rangle \quad \text{(velocity form)}, \tag{3}$$

*Project supported by the National Natural Science Foundation of China (Grant No 19974028).

†Author to whom correspondence should be addressed. Tel: 028-85405526(O), 85408258(H); E-mail: biophoton@163.com

where $\psi_0$ and $\psi_f$ are the exact initial and final electric wavefunctions, and $E_0$ and $E_f$ are the exact energy eigenvalues of $H$ corresponding to $\psi_0$ and $\psi_f$. In the lowest order, $\psi_0$ becomes the unperturbed ground state $\Phi_0$, which is given by

$$H_0 \Phi_0 = E_0^{(0)} \Phi_0, \tag{4}$$

$$\text{in which} \quad H_0 = \sum_{i=1}^{N} \left[ -\frac{\nabla_i^2}{2} - \frac{Z}{r_i} + V(r_i) \right] \tag{5}$$

$$\text{and} \quad H_c = \sum_{i<j=1}^{N} \nu_{ij} - \sum_{i=1}^{N} V(r_i), \tag{6}$$

where $V(r_i)$ accounts for the average interaction of the $i$th electron with the remaining $N-1$ electrons, and $H_c$ is the electron-correlation perturbation.

In the MBPT, dipole matrices $Z_L$ and $Z_V$ can be represented by a series of diagrams, some of which are shown in Fig.1.

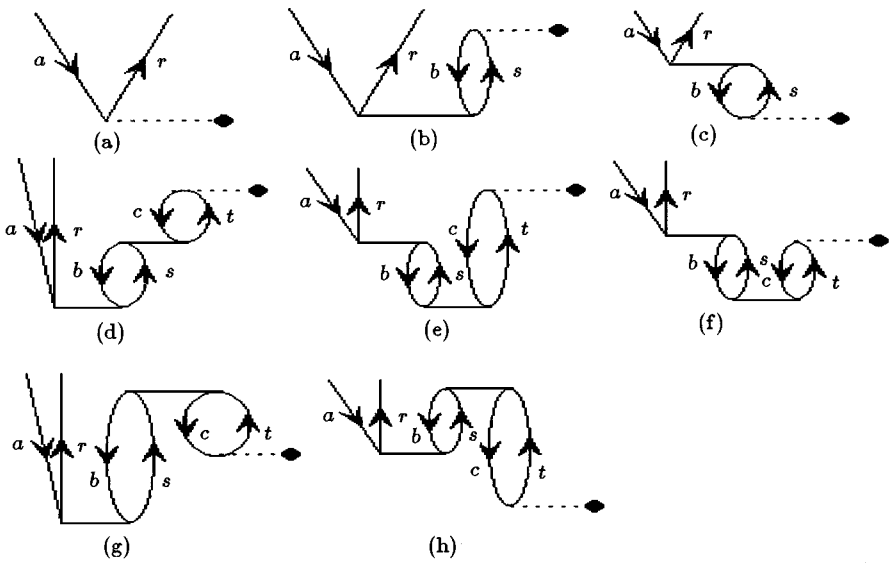



**Fig.1.** Brueckner–Goldstone diagrams contributing to the dipole matrix element of photoionization. The dashed lines ending with a dot indicate the matrix elements of the dipole operator $z$ (length form) or $\mathrm{d}/\mathrm{d}z$ (velocity form). The solid lines represent Coulomb interactions. The labels $a$, $b$, $c$ represent the ground-state orbitals and $r$, $s$ and $t$ represent the excited orbitals.

Figure 1(a) is the lowest-order contribution. The first-order GSC and the final-state correlation(FSC) are given by Figs.1(b) and 1(c) respectively. Figures 1(d)–(f) represent the second-order GSC, and Figs.1(g) and (h) are the second-order RPA. All these diagrams are read from bottom to top corresponding to right to left in $\left\langle \psi_f \middle| \sum z_i \middle| \psi_0 \right\rangle$. The expressions for Figs.1(d) and (e) are

$$\frac{\langle \nu \rangle_{\mathrm{arbs}} \langle \nu \rangle_{\mathrm{bsct}} \langle z \rangle_{\mathrm{ct}}}{(\varepsilon_a - \varepsilon_r + \varepsilon_b - \varepsilon_s)(\varepsilon_a - \varepsilon_r + \varepsilon_c - \varepsilon_t)} \tag{7}$$

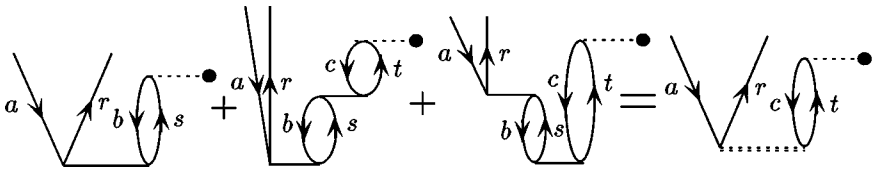
and

$$\frac{\langle \nu \rangle_{\mathrm{arbs}} \langle \nu \rangle_{\mathrm{bsct}} \langle z \rangle_{\mathrm{ct}}}{(\varepsilon_b - \varepsilon_s + \varepsilon_c - \varepsilon_t)(\varepsilon_a - \varepsilon_r + \varepsilon_c - \varepsilon_t)} \tag{8}$$

respectively, where $a$, $b$ and $c$ are core orbitals, and $r$, $s$ and $t$ run over all the bound or continuum excited orbitals. Comparing with the formula for the first-order GSC

$$\frac{\langle \nu \rangle_{\mathrm{arct}} \langle z \rangle_{\mathrm{ct}}}{(\varepsilon_a - \varepsilon_r + \varepsilon_c - \varepsilon_t)}, \tag{9}$$

and factoring out the common part in Eqs.(7)–(9), we have




$$= \left[\langle\nu\rangle_{\rm arct} + (\langle\nu\rangle_{\rm arbs}\langle\nu\rangle_{\rm bsct})\left(\frac{1}{(\varepsilon_a - \varepsilon_r + \varepsilon_b - \varepsilon_s)} + \frac{1}{(\varepsilon_b - \varepsilon_s + \varepsilon_c - \varepsilon_t)}\right)\right]\frac{\langle z\rangle_{\rm ct}}{(\varepsilon_a - \varepsilon_r + \varepsilon_c - \varepsilon_t)}. \qquad (10)$$

Thus, the second-order GSC can be treated together with the first-order GSC and can be taken as if it were a correction to the Coulomb interaction of the first-order GSC. The effect of these two diagrams will be discussed in detail in section 3.

## 3. Results and discussion

The contribution to the cross section from the single photoionization transitions of 1s$\rightarrow k$l, 2s$\rightarrow k$l, 2p$\rightarrow k$l, and 3s$\rightarrow k$l is very small, so we just consider the main transition channels, such as 3p$\rightarrow k$d, 3p$\rightarrow k$s, 3d$\rightarrow k$p, 3d$\rightarrow d$f, and 4s$\rightarrow k$p in the second-order GSC and RPA correlations. All the channels are listed in Table 1. The ionization energies for 4s and 3d subshells are taken from Ref.[8] and other energy values used in this work are adopted from Ref.[1]. In this paper, ground-state orbits are calculated by using the computer program MCHF77 of Froese Fischer.[9] We adopt MARFUL and MYBOUND by Kelly to calculate the continuum states and bound states respectively.

**Table 1.** Transition channels and ionization energies.

| Transition | Abb. | Ionization energy $E_{\rm i}$/eV |
|---|---|---|
| $3p^6 3d^5 4s^2 \rightarrow 3d^6 3d^5 4s\varepsilon p$ | 4s$\rightarrow \varepsilon$p | 7.434 |
| $3p^6 3d^5 4s^2 \rightarrow 3d^6 3d^4(^5D) 4s^2 \varepsilon f$ | 3d$\rightarrow \varepsilon$f | 14.299 |
| $3p^6 3d^5 4s^2 \rightarrow 3d^6 3d^4(^5D) 4s^2 \varepsilon p$ | 3d$\rightarrow \varepsilon$p | 14.299 |
| $3p^6 3d^5 4s^2 \rightarrow 3d^5 3d^5 4s^2 \varepsilon d$ | 3p$\rightarrow \varepsilon$d | 57.058 |
| $3p^6 3d^5 4s^2 \rightarrow 3d^5 3d^5 4s^2 \varepsilon s$ | 3p$\rightarrow \varepsilon$s | 73.899 |

We present the results in Fig.2 for the cross section of the photoionization 3d$\rightarrow k$f in both length and velocity forms. In Fig.2 (a), we do not include the second-order GSC and RPA correlations. We can find that in the low-energy region, there is a large discrepancy between the results of the length and velocity forms. When the second-order GSC is added, the results are modified and excellent agreement between them is realized. From Eq.(10), the second-order GSC can be treated together with the first-order GSC and can be taken as if it were a correction to the Coulomb interaction of the first-order GSC. Usually, the first-order GSC diagram of Fig.1(b) decreases the magnitude of the velocity cross section so much that the length-velocity discrepancy increases. When the second-order GSC diagrams of Figs.1(d)–(f) are included, they moderate the overestimated effect by Fig.1(b) and improve the length-velocity agreement very much.

The photoionization cross section of 3p subshell is shown in Fig.3 together with the experimental results of Jiménez-Mier *et al*[1] and theoretical result of Yeh and Lindau.[2] In Ref.[1], a Cooper minimum occurs at about 100eV. In contrast, Ref.[2] gives the minimum at about 80eV. Our MBPT calculation gives the minimum at 93.7eV, which is much closer to the experimental results than other theoretical calculations. We find that there is a large discrepancy between our calculation and the experimental results[1] in low-energy region. This is because the big resonance 3p$\rightarrow$3d gives a very strong interaction with the photoionization 3p$\rightarrow k$l. But we do not consider this interaction in this paper, and we will calculate it in our next work.

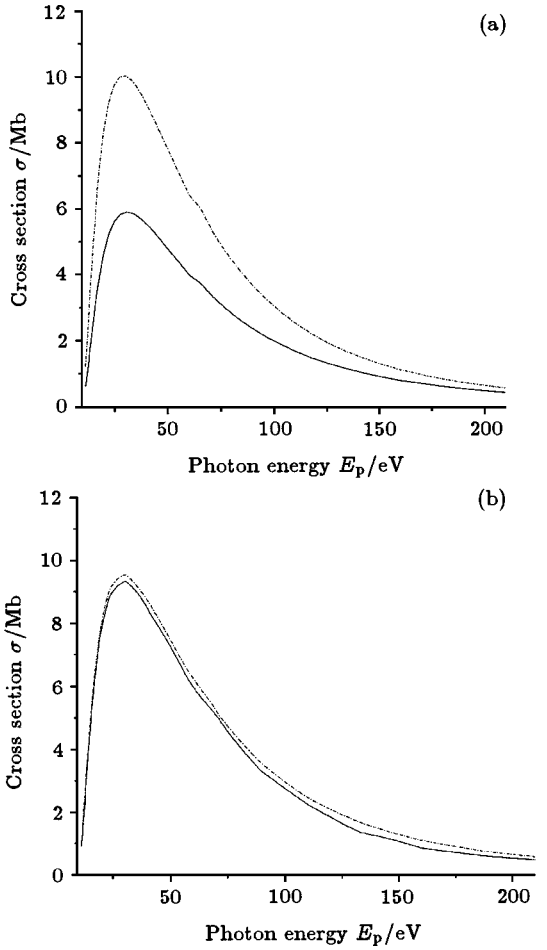



**Fig.2.** The effect of the second-order GSC and RPA correlations on the 3d→ $k$f cross section. (a) The lowest order; (b) adding the second-order GSC and RPA correlation.

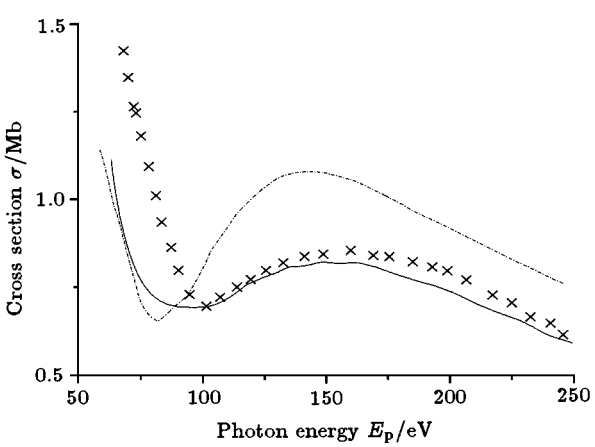



**Fig.3.** Partial cross section for the photoionization of 3p subshell. Theoretical calculations: solid line, this work(MBPT); dot-dashed line, Ref.[2] (HS). Experimental results: cross, from Ref.[1].

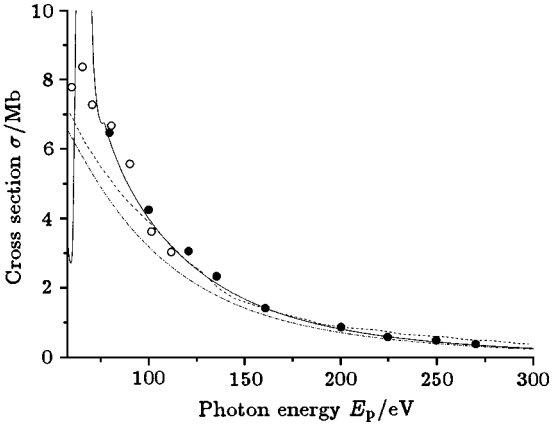



**Fig.4.** Partial cross section for the photoionization of 3d subshell. Theoretical calculations: solid line, this work(MBPT); dashed line, Ref.2(HS); dot-dashed line, this work(MBPT only including the lowest order). Experimental results: circle, Ref.[10]; and black dot, Ref.[1].

In Fig.4, we present the results of the partial 3d cross section. The solid line connects the HS results in Ref.[2]. The other two experimental results are taken from Refs.[1] and [9]. To gain the 3d partial cross section, we add two channels of 3d→ $k$f and 3d→ $k$p. In higher-energy regions, both theoretical calculations are in excellent agreement with the experimental results. Our calculations are more suitable than the HS results for lower photon energies. To show the effect of RPA, we also give the lowest order of MBPT, which gives almost the same results as those in Ref.[2].

The turning point on the line with circles near 58eV in Fig.4 is caused by the 3p→3d resonance, and is replicated by our MBPT correctly, but we are not going to discuss this structure here. This phenomenon will be studied in detail in a future paper.

We can see that, because a single-particle description is used to generate core orbitals, the second-order GSC diagrams should be included to correct the core orbitals. We have found that the first-order GSC affects the velocity form of cross sections strongly. With incomplete GSC diagrams the length-velocity agreement may not be achieved. Hence, the higher-order GSC diagrams should be taken into account. We take into account the second-order GSC for the photoionization cross section and improve the length-velocity agreement significantly.

## 4. Conclusion

The second-order GSC and RPA diagrams are included in our calculation of photoionization cross sections for manganese. We take the screening effect produced by other electrons into account and modify the strength of interaction between the involved electrons. Our discussion for the second-order GSC and RPA correlations is successful. Our calculation gives excellent agreement between the length and velocity forms of cross sections. For 3p partial cross sections, our MBPT is more reasonable than other theoretical calculations, and the location of Cooper minimum can be compared with the experimental results. For 3d partial cross sections, our calculations agree excellently with the experimental results.

In conclusion, we have found that the second-order GSC and RPA correlations play a key role in calculating the partial cross sections, and MBPT is still useful in dealing with the inner-shell photoionization of neutral atoms.

## References

[1] Jiménez-Mier J, Krause M O and Gerard P 1989 *Phys. Rev.* A **40** 3712
[2] Yeh J J and Lindau I 1985 *At. Data Nucl. Data Tables* **32** 1
[3] Liu J C, Liu H K, Wang Z L, Cheng Y S and Yang X D 1998 *J. Phys.* B **31** L553
[4] Pu F N, Liu J C and Cheng Y S 2000 *J. Phys. B: At. Mol. Opt. Phys.* **33** 1203
[5] Jiang D Q, Liu J C, Yang X D and Lu P F 2001 *Phys. Lett.* A **288** 95
[6] Cheng Y S, Liu J C and Sun W G 1998 *Acta. Phys. Sin.* (Overseas Edition) **7** 161
[7] Garvin L J, Brown E R, Carter S L and Kelly H P 1983 *J. Phys. B: At. Mol. Opt. Phys.* **16** L269
[8] Moore C E 1949 *Atomic Energy Levels* NBS Circular No 467
[9] Froese Fischer C 1978 *Comput. Phys. Commun.* **14** 1
[10] Krause M O, Carlson T A and Fahlman A 1984 *Phys. Rev.* A **30** 1316